

Slow polarization relaxation in water observed by hyper-Rayleigh scattering

David P. Shelton*

Physics Department, University of Nevada, Las Vegas, Nevada 89154-4002, USA

(Received 25 March 2005; published 15 July 2005)

Polar fluctuations due to reorientation of the dipolar molecules in liquid water are central to its properties. Here we report a high resolution hyper-Rayleigh light-scattering spectrum for liquid water which shows collective dipole orientation fluctuations on two very different time scales: 10 ps and >50 ns. The 10 ps relaxation time for the transverse fluctuations matches the macroscopic dielectric relaxation time, but the >50 ns relaxation time for the longitudinal fluctuations has not been previously observed and is dramatically ($10^5\times$) slower than expected.

DOI: [10.1103/PhysRevB.72.020201](https://doi.org/10.1103/PhysRevB.72.020201)

PACS number(s): 78.35.+c, 33.20.Fb, 61.20.Lc, 77.22.Gm

The molecular dynamics and structure of liquid water are of fundamental importance in chemistry and biology, but many aspects of water remain a subject of debate despite extensive study. Liquid water is thought to have a hydrogen-bonded network structure, based on evidence from neutron and x-ray diffraction, infrared spectroscopy, and molecular-dynamics simulations. However, recent experiments^{1,2} find serious discrepancies with structures based on current molecular-dynamics simulations, which reinforces the need for unambiguous experimental measurements. The angular correlations and dynamics of the molecules in water are difficult to study by the usual neutron, x-ray, light scattering, and NMR techniques. The depolarized light-scattering spectrum for anisotropic molecules usually carries direct information about orientational dynamics: the rotation frequency of molecules in the gas phase and the reorientation rate for molecules in the liquid. This is not the case for water, since the polarizability of the water molecule is nearly isotropic. Depolarized light scattering and optical Kerr effect signals for water are dominated by intermolecular collision-induced contributions, mediated by the dipole-induced-dipole (DID) mechanism.³ Second harmonic or hyper-Rayleigh light scattering (HRS) is a probe that is sensitive only to the polar fluctuations in a liquid, and provides direct information about the orientational dynamics of the molecules in water.

Hyper-Rayleigh scattering⁴⁻⁸ is mediated by the third rank molecular hyperpolarizability β . HRS probes noncentrosymmetric fluctuations such as orientation fluctuations of polar molecules and vanishes for modes of even parity such as density fluctuations. The HRS spectrum for water is most sensitive to dipolar orientational fluctuations since β of the water molecule is dominated by its dipolar irreducible spherical tensor component.⁸ The HRS spectrum probes fluctuations with wave vector $\mathbf{k}=2\mathbf{k}_i-\mathbf{k}_s$, where \mathbf{k}_i and \mathbf{k}_s are the wave vectors of the incident and scattered photons, respectively. For 90° scattering of linearly polarized light one polarized intensity I_{VV} and three depolarized intensities I_{HV} , I_{VH} , and I_{HH} may be measured, where the first and second subscripts refer to the linear polarizations of the incident and scattered light with respect to the horizontal scattering plane, respectively. In the case of randomly oriented molecules the HRS intensity is the incoherent sum of the scattering from the individual molecules, and the HRS intensities for the three depolarized scattering geometries are identical by sym-

metry. This symmetry is broken for HRS from polar molecules with a preferred orientation.⁹ The ratio of depolarized HRS intensities is $I_{HV}/I_{VH}=0$ for molecules polarized in the direction of the scattering vector \mathbf{k} (longitudinal, L), and $I_{HV}/I_{VH}=2$ for molecules polarized perpendicular to the scattering vector (transverse, T). The symmetric result $I_{HV}/I_{VH}=1$ is recovered for the integrated intensity when the amplitudes of the longitudinal mode and each of the two transverse modes are equal. The symmetric result $I_{HV}/I_{VH}=1$ is obtained at every point in the spectrum also when the spectral widths of the longitudinal and transverse modes are equal.

Previous low resolution measurements of the VV , HV , and VH HRS spectra for water^{5,8} found a peak centered at the second harmonic wavelength, with spectral width $2\Delta\nu=1.0\text{ cm}^{-1}$ (full width at half maximum intensity, FWHM) at $T=23^\circ\text{C}$. The corresponding orientational relaxation time $\tau=(2\pi\Delta\nu)^{-1}$ is 10.6 ps at 23°C , decreasing to 3.6 ps at 80°C . At all temperatures the spectral intensity ratio I_{HV}/I_{VH} did not equal 1, and the spectra were fit by allowing L and T components with different spectral widths but also with similar integrated intensity. Due to the low spectral resolution in those experiments, only an upper bound of 0.3 cm^{-1} could be established for the spectral width of the narrow L component of the VH spectrum. In the present work we modified the previously described apparatus⁸ to observe the VH HRS spectrum of D_2O at higher resolution. The laser was injection seeded to produce single-longitudinal-mode output pulses at $\lambda=1064\text{ nm}$, and a confocal Fabry-Perot interferometer with 1.0 GHz free spectral range was added in series with the grating spectrometer. The spectral response function of the instrument (reference spectrum) was measured by back-lighting the sample with second harmonic light generated in a potassium titanyl phosphate (KTP) crystal. The HRS spectrum and the reference spectrum were recorded on alternate scans of the interferometer for 3.6×10^5 scans of 2 s duration. The laser pulses (0.8 mJ, 90 ns, 2.2 kHz repetition rate) were focused to a $15\text{-}\mu\text{m}$ -diam beam waist in the sample, giving 0.016 count/s peak HRS signal as compared to the 7×10^{-4} count/s gated dark count rate.

Figure 1 shows the high resolution VH HRS spectrum for liquid D_2O at $T=25^\circ\text{C}$. It consists of a narrow peak riding

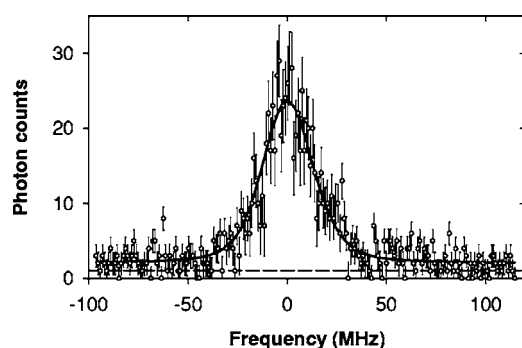


FIG. 1. High-resolution VH HRS spectrum measured for D_2O at $T=25$ °C. The error bars on the data points are 1 S.D. The solid curve is the least squares fit of the 30 MHz wide instrument response function convolved with a very narrow Lorentzian plus a constant background, and the dashed line marks the dark count of the detector.

on a flat background. The curve fitted to the observed spectrum is the sum of a constant background term and a peak which is the convolution of the reference spectrum with a Lorentzian function $f(\nu)=A/[1+(\nu/\Delta\nu)^2]$ representing the L component of the HRS spectrum. The weighted least squares fit to the data gives $2\Delta\nu=0.5\pm 2.0$ MHz (1 S.D.) for the Lorentzian, much narrower than the 30 MHz width of the reference spectrum. At the 99% confidence level the width of the narrow HRS component is <6.5 MHz. The background is composed of approximately equal contributions from the broad HRS component of width $1.1\text{ cm}^{-1}=33$ GHz at 25 °C (Ref. 8) and from the detector dark count (shown as the dashed horizontal line). The apparent intensity of the broad HRS component is increased by an overlap of 90 spectral orders of the Fabry-Perot interferometer which fall within the 3 cm^{-1} spectral window selected by the grating spectrometer. The ratio of integrated intensities for the narrow and wide VH HRS components obtained from this spectrum is 0.62 ± 0.10 , in agreement with 0.52 ± 0.10 obtained from the previous experiment.⁸

Figure 2 shows the VV, HV, and VH HRS spectra for water calculated by combining the results of this experiment with the previous lower resolution measurements. As previously described,⁸ each spectrum is the sum of four compo-

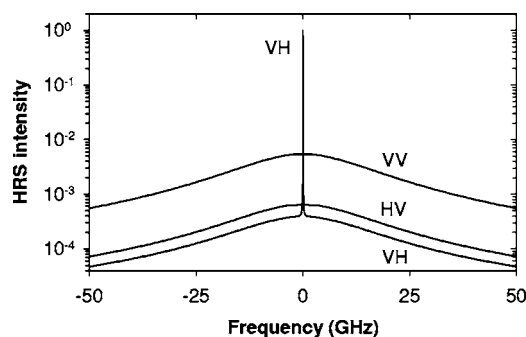


FIG. 2. Comparison of VV, HV, and VH HRS spectral intensities for D_2O at $T=25$ °C. The narrow spike due to the slowly relaxing L mode is present only in the VH spectrum. The spectra are normalized to unit peak height for the VH spectrum.

nents distinguished by their polarization dependence: a very broad and low DID component, intermediate width isotropic and transverse components, and a narrow longitudinal component. Figure 2 is composed using the integrated intensities, widths, and spectral functions from the previous work,⁸ except for the spectral width of the L component which is obtained from the present work. In Fig. 2 the width of the L component is set to the 6.5 MHz upper bound determined from this experiment. The corresponding relaxation time is 50 ns, which is 5000 times slower than the relaxation time for the T component, and 3 times slower than the relaxation time for thermal fluctuations with the same k in water (Rayleigh peak width 22 MHz). Although a difference in relaxation times for the L and T components is allowed since they are distinguished by their molecular polarization with respect to the scattering vector, the extreme observed difference is surprising.

In the present work deuterated water D_2O was studied for the reason that it produces a larger HRS signal than H_2O due to the reduced absorption and thermal defocusing of the near-infrared laser beam in the sample. Other than the smaller signal, the low resolution VV, HV, and VH HRS spectra for H_2O are similar to the D_2O spectra, including a narrow component in the VH spectrum alone. Furthermore, the narrow VH component has also been observed in low-resolution HRS spectra for the dipolar liquid acetonitrile, so this phenomenon is not restricted to water. Conversely, a narrow VH component is not observed in the HRS spectrum of the nonpolar liquid CCl_4 .

The VH HRS spectrum is the Fourier transform of the time correlation function

$$\left\langle \sum_{a,b} \beta_{xyy}(r_a, \Omega_a, t) \beta_{xyy}(r_b, \Omega_b, t + \tau) \cos(\Delta k \cdot r_{ab}) \right\rangle,$$

where the sum extends over all molecules in the sample, and β_{xyy} is the lab frame component of the molecular hyperpolarizability tensor with x the incident beam direction and z the observation direction.⁴⁻⁶ For water the β tensor is dominated by its first rank irreducible spherical tensor part,⁸ which transforms the same as the dipole moment for molecular rotations. Therefore, the dynamics governing HRS from water are nearly the same as for reorientation of the dipole moment, and HRS orientational relaxation times for water may be compared to dielectric relaxation times since both are due to fluctuations of the collective dipole moment density. The transverse dielectric relaxation time for water at $T=25$ °C measured by THz reflection spectroscopy is 8.8 ps for D_2O and 7.1 ps for H_2O ,¹⁰ and that measured by 9.6 GHz dielectric spectroscopy is 8.0 ps for H_2O .¹¹ These results are close to the 9.6 ps relaxation time for the T component of the HRS spectrum for D_2O at 25 °C. Although the dielectric measurements were made near the $k=0$ limit ($k < 500\text{ cm}^{-1}$) while the HRS measurements probe fluctuations with $k=2.2 \times 10^5\text{ cm}^{-1}$ (wavelength 280 nm), the dielectric and HRS relaxation times should agree since the transverse dielectric function is a smooth function that is nearly k independent for small k .

The explanation of the longitudinal HRS relaxation time is more problematic. Although molecular-dynamics simula-

tions for water^{12,13} and other polar liquids^{14–18} show different behavior for the T and L components of the dielectric function $\varepsilon(\mathbf{k}, \omega)$, the longitudinal dipole density is related to $[1 - 1/\varepsilon_L(\mathbf{k}, \omega)]$ which is well behaved and slowly varying for small k , and no singularity is expected for τ_L . Furthermore, there is a theoretical argument¹⁹ based on the assumption of a linear isotropic constitutive relation $D = \varepsilon E$, which predicts that the longitudinal dipole density relaxation at small k will be *faster* than the transverse relaxation by a factor $\varepsilon_0/\varepsilon_\infty \approx 80/1.7 = 47$ for water, in obvious contradiction with the present experimental results. An extensively investigated class of models for polar liquids consists of dipolar point particles interacting by the sum of dipole and short-range spherical potentials.^{20–28} These models exhibit a rich variety of structures and dynamic collective effects such as strong longitudinal dipole oscillations at low k and orienta-

tional ordered fluid phases, but make no prediction for the results of this experiment. In summary, existing theory does not account for the slow relaxation observed in the present experiment.

The main finding of this work is that the longitudinal orientational polarization relaxation in water is $>5,000$ times slower than the transverse relaxation for fluctuations with wavelength 280 nm. The longitudinal orientational polarization relaxation time observed by HRS in water differs from the theoretical prediction by five orders of magnitude and is not presently understood.

The author thanks Bill O'Donnell and Doug Fettig for their technical assistance and the referees for their comments.

*Email address: shelton@physics.unlv.edu

¹Y. Zubavicus and M. Grunze, *Science* **304**, 974 (2004).

²Ph. Wernet *et al.*, *Science* **304**, 995 (2004).

³V. Mazzacurati, A. Nucara, M. A. Ricci, G. Ruocco, and G. Signorelli, *J. Chem. Phys.* **93**, 7767 (1990).

⁴R. Bersohn, Y.-H. Pao, and H. L. Frisch, *J. Chem. Phys.* **45**, 3184 (1966).

⁵P. D. Maker, *Phys. Rev. A* **1**, 923 (1970).

⁶S. Kielich, in *Progress in Optics*, edited by E. Wolf (North-Holland, Amsterdam, 1983), Vol. XX, p. 155.

⁷V. N. Denisov, B. N. Mavrin, and V. B. Podobedov, *Phys. Rep.* **151**, 1 (1987).

⁸D. P. Shelton, *J. Chem. Phys.* **117**, 9374 (2002); **121**, 3349 (2004).

⁹D. P. Shelton, *J. Opt. Soc. Am. B* **17**, 2032 (2000).

¹⁰C. Ronne, P.-O. Astrand, and S. R. Keiding, *Phys. Rev. Lett.* **82**, 2888 (1999).

¹¹D. Bertolini, M. Cassettari, and G. Salvetti, *J. Chem. Phys.* **76**, 3285 (1982).

¹²P. A. Bopp, A. A. Kornyshev, and G. Sutmann, *J. Chem. Phys.* **109**, 1939 (1998).

¹³D. Bertolini and A. Tani, *Mol. Phys.* **75**, 1065 (1992).

¹⁴B.-C. Perng and B. M. Ladanyi, *J. Chem. Phys.* **110**, 6389 (1999).

¹⁵B. M. Ladanyi and M. S. Skaf, *J. Chem. Phys.* **100**, 1368 (1996).

¹⁶M. S. Skaf, T. Fonseca, and B. M. Ladanyi, *J. Chem. Phys.* **98**, 8929 (1993).

¹⁷T. Fonseca and B. M. Ladanyi, *J. Chem. Phys.* **93**, 8148 (1990).

¹⁸D. M. F. Edwards, P. A. Madden, and I. R. McDonald, *Mol. Phys.* **51**, 1141 (1984).

¹⁹D. Kivelson and H. L. Friedman, *J. Phys. Chem.* **93**, 7026 (1989).

²⁰E. L. Pollock and B. J. Alder, *Phys. Rev. Lett.* **46**, 950 (1981).

²¹M. Neumann, *Mol. Phys.* **57**, 97 (1986).

²²M. J. Stevens and G. S. Grest, *Phys. Rev. E* **51**, 5962 (1995).

²³B. Groh and S. Dietrich, *Phys. Rev. E* **53**, 2509 (1996).

²⁴B. Groh and S. Dietrich, *Phys. Rev. E* **55**, 2892 (1997).

²⁵B. Groh and S. Dietrich, *Phys. Rev. Lett.* **79**, 749 (1997).

²⁶I. P. Omelyan, I. M. Mryglod, and M. V. Tokarchuk, *Phys. Rev. E* **57**, 6667 (1998).

²⁷V. V. Murashov, P. J. Camp, and G. N. Patey, *J. Chem. Phys.* **116**, 6731 (2002).

²⁸G. M. Range and S. H. L. Klapp, *Phys. Rev. E* **70**, 031201 (2004).